

Instability, unfolding and aggregation of human lysozyme variants underlying amyloid fibrillogenesis

David R. Booth*^{||}, Margaret Sunde^{†||}, Vittorio Bellotti*[‡], Carol V. Robinson[‡], Winston L. Hutchinson*, Paul E. Fraser[§], Philip N. Hawkins[‡], Christopher M. Dobson[‡], Sheena E. Radford^{‡‡}, Colin C. F. Blake[†] & Mark B. Pepys^{*}

* Immunological Medicine Unit, Royal Postgraduate Medical School, Hammersmith Hospital, London W12 0NN, UK

† Laboratory of Molecular Biophysics and ‡ New Chemistry Laboratory, Oxford Centre for Molecular Sciences, University of Oxford, Oxford OX1 3QT, UK

§ Centre for Research in Neurodegenerative Diseases, University of Toronto, Toronto M5S 3H2, Canada

|| These authors contributed equally to this work.

Tissue deposition of soluble proteins as amyloid fibrils underlies a range of fatal diseases. The two naturally occurring human lysozyme variants are both amyloidogenic, and are shown here to be unstable. They aggregate to form amyloid fibrils with transformation of the mainly helical native fold, observed in crystal structures, to the amyloid fibril cross- β fold. Biophysical studies suggest that partly folded intermediates are involved in fibrillogenesis, and this may be relevant to amyloidosis generally.

Tissue deposition of soluble autologous proteins as insoluble amyloid fibrils is associated with serious diseases including systemic amyloidosis, Alzheimer's disease, and transmissible spongiform encephalopathy, but the mechanisms of amyloid fibrillogenesis are poorly understood¹. Although the diverse human proteins that can form amyloid fibrils *in vivo* have unrelated sequences and tertiary folds, they can all polymerize into fibrils with similar ultrastructural appearance and identical tinctorial properties². Furthermore, the core structure of all amyloid fibrils consists of β -sheets with the strands perpendicular to the long axis of the fibre^{3,4}. Knowing which conformational rearrangements converge on the same final fold is important for understanding the determinants of protein structure, and may enable the development of rational approaches to the treatment of amyloid diseases. However, although a lot is known about the mutations and substitutions responsible for hereditary and acquired amyloidosis (see, for example, refs 5–14), there is little detailed information about the relationship between structure and folding in amyloid proteins.

The two known natural mutations in the human lysozyme gene both cause autosomal dominant hereditary amyloidosis¹⁵. Affected individuals are heterozygous for single base changes which encode non-conservative amino-acid substitutions, Ile56Thr and Asp67His, respectively, and the amyloid fibrils consist exclusively of the variant protein¹⁵ (see below). The structure, dynamics and folding of c-type lysozymes and the related α -lactalbumins have been studied comprehensively^{16–23}. The identification of lysozyme as an amyloidogenic protein was therefore of particular interest.

Here we present a detailed analysis of the structure, stability, conformational dynamics and fibrillogenic properties of the amyloidogenic lysozyme variants which links the formation of amyloid with the folding behaviour of proteins.

Amyloidogenic variants have native folds

Wild-type lysozyme and the amyloidogenic variants¹⁵, which have

Table 1 Molecular masses and enzyme characteristics of wild-type and variant lysozymes

Protein	Electrospray ionization mass spectrometry		Enzyme properties	
	Observed M_r	Predicted M_r	K_M (μ M)	k_{cat} ($M s^{-1}$)
Natural wild type	14,691	14,693	not done	not done
Recombinant wild type	14,696	14,693	16.5 (4)	14.5 (0.5)
Recombinant Ile56Thr	14,681	14,680	18.5 (3)	15.0 (0.5)
Recombinant Asp67His	14,718	14,715	38.0 (9)	9.5 (0.5)

K_M and k_{cat} are given as mean (s.d.).

not previously been isolated, were produced in the baculovirus expression system, and the correct mass of each purified, recombinant protein was demonstrated by electrospray ionization mass spectrometry²⁴ (ESI-MS) (Table 1). They were all enzymatically active, although the Asp67His variant had a higher K_M and lower k_{cat} than the wild type and the Ile56Thr variant (Table 1).

The native folds of the two amyloidogenic variants determined by X-ray crystallography both resemble that of the wild-type protein¹⁸ (Fig. 1a), and all have the four correct, intact disulphide bonds. However, substitution of Asp 67 by histidine destroys the network of hydrogen bonds that stabilizes the β -domain, resulting in a large, concerted movement of the β -sheet and the long loop within the β -domain away from each other, distortion of the active site, and an overall displacement of backbone atoms in the vicinity of residues 48 and 70 by as much as 11 Å (Fig. 1a). The crystal structure of the Ile56Thr variant does not show such changes, indicating that the movements in the β -domain are not the direct cause of amyloidogenicity. However, closer inspection of the two structures demonstrates that subtle, but structurally significant, changes at the interface region between the α - and β -domains occur in both variants (Fig. 1b, c). Ile 56 is a pivotal residue for the structural integrity of the lysozyme fold in that it links the two domains; its importance is emphasized by its high conservation in the lysozyme sequences¹⁹. An increased B-factor (11.7 Å²) was found for the C α

† Present addresses: Dipartimento di Biochimica, Università di Pavia, Via Taramelli 3B, 27100 Pavia, Italy (V.B.); Department of Biochemistry and Molecular Biology, University of Leeds, Leeds LS2 9JT, UK (S.E.R.).

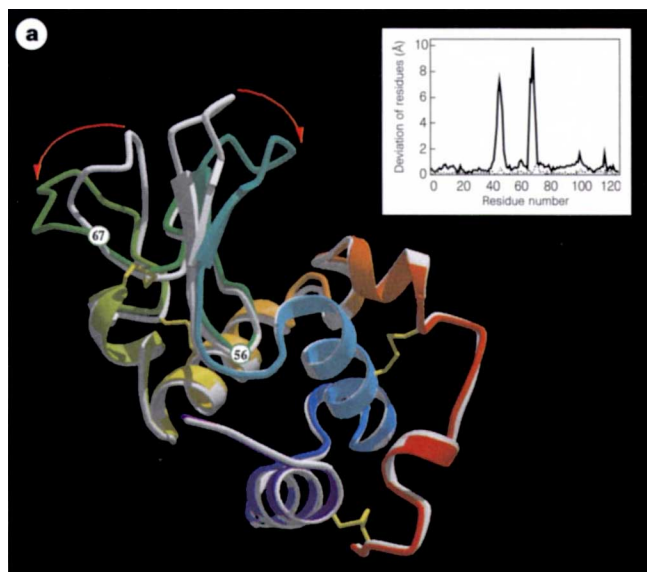
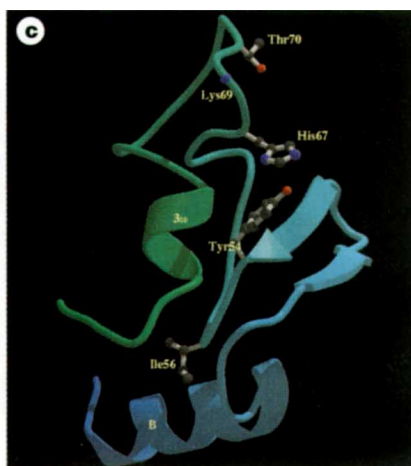
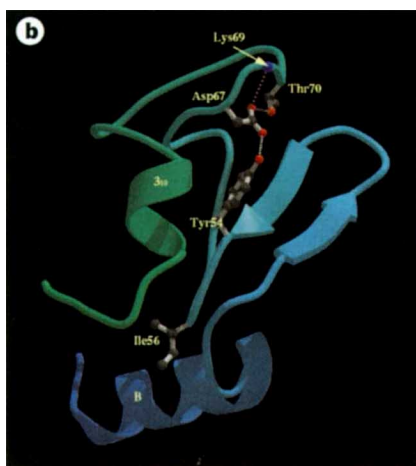


Figure 1 a, Overlay of ribbon diagrams representing the structures of wild-type human lysozyme (grey) and the soluble form of Asp67His lysozyme (coloured from blue at the N terminus to red at the C terminus). Red arrows indicate the relative movement in the positions of residues 45–54 and 67–75 in the Asp67His variant compared with those in the wild-type protein. The four native disulphide bonds in the wild-type protein and both variant structures are shown in yellow. Inset, plot showing the displacement of the residues of the Asp67His (solid line) and Ile56Thr (broken line) variants from their positions in the wild-type protein. **b**, Ribbon diagram of the β -domain of the wild-type protein, showing the critical role of Asp 67 in the network of hydrogen bonds that stabilizes this domain. **c**, Ribbon diagram illustrating the same region in the Asp67His variant and the disruption of the domain that occurs when the aspartate at position 67 is replaced by histidine and the hydrogen-bonding network is destroyed.



atom of residue 56 in the Ile56Thr variant, relative to that of Ile 56 in the wild-type protein (6.4 \AA^2). This is presumably due to the now hydrophilic side chain being in an unfavourable hydrophobic environment, even though its hydrogen-bonding potential seems to be at least partly satisfied by a hydrogen bond (length 3.3 \AA) to one of the water molecules found in both the wild-type and the variant structures. In the Asp67His variant, the changes in the conformations of the β -sheet and long loop are transmitted down to residue 56, resulting in a new orientation for the side chain and an increase in the B -factor of the $C\alpha$ atom of the latter (9.7 \AA^2). This suggests that the crucial interface region between the α - and β -domains is less constrained in both variants than in the wild-type protein. This common feature of both structures implies that it could be an important factor in their amyloidogenic properties. Substitution of Ile 55 in hen lysozyme (the corresponding residue to Ile 56 in human lysozyme) by threonine also reduces the stability of the protein and generates a tendency to aggregate²⁵, further supporting the view that this residue is essential for the maintenance of the lysozyme fold.

Fibril formation occurs *in vitro*

In contrast to the reversible thermal denaturation of wild-type lysozyme from both natural and recombinant sources, the amyloidogenic variants were inactivated by heating (Fig. 2). The variants were also less stable than wild-type lysozyme, with unfolding transition midpoints reproducibly 10°C or more below that of

the wild-type protein. Furthermore, both variants eventually lost all activity when incubated at pH 7.4 at the physiological temperature of 37°C , whereas the wild-type protein retained full activity under these conditions (data not shown).

The amyloidogenic lysozyme variants also aggregated on heating, unlike the wild-type protein. The rate and extent of aggregation varied with protein concentration and the expression batch, and although the aggregates stained with Congo red²⁶, they generally did not give the green–red birefringence in polarized light that is pathognomonic of amyloid. Nevertheless, negatively stained electron micrographs revealed rigid, non-branching fibres of indeterminate length and approximately 8–10 nm diameter, with the typical appearance of amyloid fibrils. Fibrils were also seen in electron micrographs of the sediment that formed spontaneously at 4°C in concentrated solutions of both Ile56Thr and Asp67His variants (Fig. 3). Strikingly, one preparation of heated Asp67His lysozyme contained fibres that stained with Congo red and did display the diagnostic green birefringence, confirming the capacity of the variant to form the classical amyloid structure *in vitro* independently of any other component.

Fourier-transform infrared spectroscopy (FTIR) of recombinant Asp67His lysozyme heated under conditions in which fibrils form demonstrated a predominance of β -structure and a loss of helical structure relative to the wild-type protein (Fig. 4). The FTIR spectrum also indicated the persistence of some helical structure in the heated sample. This could arise from residual soluble forms of

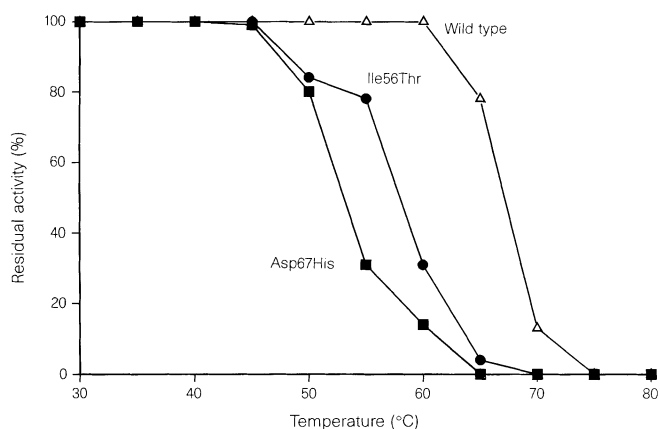


Figure 2 Melting temperatures of wild-type and amyloidogenic variant lysozymes.



Figure 3 Electron micrograph of sediment from the Ile56Thr lysozyme, after standing at 1 mg ml^{-1} for 14 days at 4°C in 10 mM HEPES, 1M LiCl, pH 8.0. Scale bar, 100 nm.

Table 2 Recovery of enzymatically active lysozyme from *ex vivo* Asp67His lysozyme amyloid fibrils

	V_e on gel filtration (ml)	Lysozyme recovered (μg)		Electrospray ionization mass spectrometry	
		Protein by A_{280}	Active enzyme	Observed M_r	Predicted M_r
<i>Ex vivo</i> Asp67His lysozyme fibrils solubilized in 6 M guanidinium-HCl, pH 6.7	13.20 (0.13)	100	80	14,716.0 14,733.8	14,715 for Asp67His lysozyme 14,729 for Asp67His lysozyme with MetSO
<i>Ex vivo</i> Asp67His lysozyme fibrils solubilized in 6 M guanidinium-HCl, pH 6.7, 0.1% 2-mercaptoethanol	12.57 (0.06)	113	0	No signal obtained	

V_e given as mean (s.d.) from 3 experiments.

the lysozyme variant, from persistence of helical structure in the fibril, or both.

Fibrillogenesis is reversible

Our identification of a second Asp67His family²⁷, apparently unrelated to the original kindred¹⁵, provided the opportunity to study Asp67His lysozyme amyloid fibrils. The X-ray fibre diffraction pattern (not shown) contains distinctive reflections at 4.6–4.8 Å on the meridian and at 8–14 Å on the equator of the image, indicating that the underlying ordered structure is a β -sheet in which the constituent β -strands are at right angles to the fibre axis¹. Such cross- β structures are characteristic of amyloid and have also been described in the glutamine repeats that are associated with several neurodegenerative diseases, including Huntington’s disease, and which cause oligomerization of proteins²⁸. The fibre diffraction pattern of *ex vivo* Asp67His lysozyme fibrils contains no reflections attributable to helical structure, suggesting that, if helices persist after transformation of the soluble protein to the fibrillar form, they are not regularly ordered.

As previously reported for Ile56Thr fibrils¹⁵, 85% of the total protein in water-extracted²⁹ Asp67His fibrils ran in reduced SDS-PAGE in the same position as intact monomeric lysozyme; the remainder consisted of oligomeric lysozyme aggregates and traces of uncharacterized high-molecular-weight material that is seen in all *ex vivo* amyloid fibrils. However, like the fibrils from the Ile56Thr case¹⁵, the Asp67His lysozyme fibrils could not be dissociated to a form detectable by ESI-MS using either acetonitrile/acetic acid mixtures or up to 100% formic acid. We therefore solubilized some of the *ex vivo* Asp67His fibrils by denaturation in 6 M guanidine HCl, isolated the lysozyme by gel filtration in the same denaturing conditions, and attempted to refold it by dialysis into water at pH

3.8, a solvent in which natural wild-type lysozyme is stable. Although some reaggregation occurred during dialysis, the recovered lysozyme was detectable by ESI-MS with a mass corresponding to intact, monomeric, Asp67His variant (Table 2). The exclusive presence of variant lysozyme in either Asp67His or Ile56Thr (ref. 15) *ex vivo* amyloid fibrils indicates that their pathological aggregation does not engage wild-type lysozyme *in vivo*, presumably because the wild type has greater stability than the variants.

Remarkably, the refolded Asp67His variant lysozyme was enzymatically active, in contrast to the absence of any activity in the original fibril preparation, using soluble penta-*N*-acetyl- β -chitopaentaoxide substrate. Although the variant protein must have undergone major conformational change *in vivo* to form characteristic cross- β amyloid fibrils, it remained able, after unfolding, to renature spontaneously into the active enzyme. However, when the disulphide bonds within the chain were reduced with 2-mercaptoethanol during solubilization and unfolding, no lysozyme activity was observed and the protein could not be detected by ESI-MS (Table 2).

Stabilized molten globule intermediate

We have used circular dichroism to monitor the unfolding behaviour of the two lysozyme variants under conditions in which they form fibrils *in vitro*. The results (Fig. 5a–d) showed that both variants were less thermostable than the wild-type protein, with midpoints of denaturation approximately 12 °C lower than that of the wild-type protein at pH 5.0. More importantly, however, the unfolding transition of the two amyloidogenic variants, although reversible under conditions in which fibril formation did not occur, was not cooperative. This resulted in a partly folded state being significantly populated near the midpoint of unfolding. This state

Table 3 Crystallographic data statistics

Parameters	Recombinant wild type	Asp67His variant	Ile56Thr variant
Structure determination			
Resolution (Å)	30–1.8 Å	30–1.75 Å	30–1.8 Å
Data completeness (%)	89.9	90.9	92.8
I/σ for all hkl	12.1	8.5	11.2
I/σ at high-resolution limit	3.7	3.1	3.6
Observations	51,285	41,333	49,524
Unique reflections	10,221	11,071	10,578
Space group	$P2_12_12_1$	$P2_1$	$P2_12_12_1$
Unit cell (Å)	56.62 × 60.88 × 33.79	37.34 × 31.86 × 51.50	56.80 × 60.89 × 33.70
β -angle		102.56°	
R_{sym} (%)	8.3	10.3	9.2
Structure refinement			
Resolution (Å)	8–1.8 Å	8–1.8 Å	8–1.8 Å
Non-H atoms	1,029	1,031	1,028
Water molecules	38	115	43
R -factor (reflections)	21.3 (10,216)	22.8 (10,216)	21.1 (10,513)
Average B -value	13.11	13.54	16.76
R.m.s.d. bond lengths (Å)	0.013	0.015	0.013
R.m.s.d. bond angles (°)	1.674	1.814	1.643
R.m.s.d. dihedral angles (°)	24.132	23.076	24.501
R.m.s.d. improper angles (°)	1.463	1.666	1.391

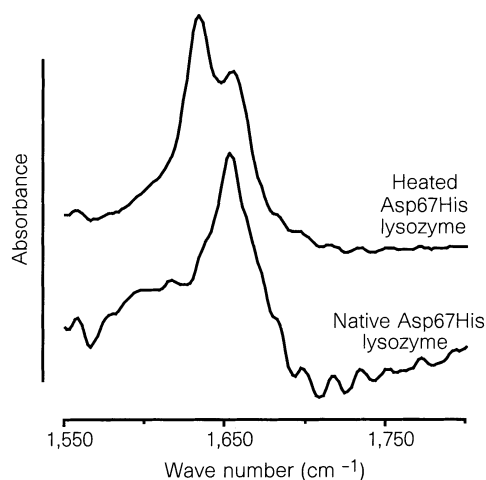


Figure 4 FTIR spectra, offset for comparison, of soluble Asp67His lysozyme, and after heating to induce fibril formation. The dominant absorption band centred at 1,655 cm^{-1} in the untreated sample reflects the large α -helical component in the soluble, native protein. The shift to absorption at about 1,630 cm^{-1} after heating indicates an increase in β -sheet content. The shoulder at 1,655 cm^{-1} in the heated sample demonstrates the persistence of some helix.

had substantial helical secondary structure but lacked persistent tertiary interactions (Fig. 5b, d). Such behaviour is quite different from the cooperative unfolding displayed by the wild-type protein under these conditions (Fig. 5a, c), but is similar to the thermal unfolding of wild-type human lysozyme under conditions of extremely low pH, where the protein unfolds through a partially structured intermediate with circular-dichroism properties similar to those identified here for the variants at pH 5.0 (ref. 30). Moreover, species with similar properties have been identified on the kinetic or equilibrium folding pathways of other lysozymes and α -lactalbumins^{21,23}. At the midpoint of thermal denaturation, the partly folded amyloidogenic intermediates bound the hydrophobic dye 1-anilino-naphthalenesulphonic acid (ANS) (Fig. 5f); this is one of the major characteristics of the previously characterized lysozyme and α -lactalbumin molten globules^{22,23}. The Ile56Thr variant also bound ANS at 20 °C, although it generated weaker

fluorescence than at its midpoint of unfolding, indicating the presence of exposed hydrophobic regions even at this temperature.

Transient unfolding

The conformational dynamics of the wild-type and variant proteins in solution at 37 °C were investigated by using ESI–MS to monitor the exchange of the labile amide and side-chain hydrogens with solvent deuterons (Fig. 6). The hydrogen exchange kinetics of the two amyloidogenic variants were remarkable in that there was very little protection from exchange (Fig. 6); in contrast, about 55 hydrogens were strongly protected from exchange in the wild-type protein under these conditions (Fig. 6). The lack of protection of the variants cannot be explained simply by their thermal destabilization relative to the wild-type protein; a chemically modified hen lysozyme, which lacks a single disulphide bridge, has a midpoint of unfolding 24 °C lower than the wild-type protein, but still shows significant protection against hydrogen exchange³². Rather, these results suggest that the alterations in the domain interface of the Ile56Thr and Asp67His variants reduce the stability and cooperativity of the native fold such that both the amplitude and frequency of the native-state fluctuations are increased, even at 37 °C, to an extent that allows solvent water access to the interior of the protein. The degree of protection of the variants is similar to that previously observed by ESI–MS in the well-characterized, partly folded, molten globule state of α -lactalbumin³³. We suggest, therefore, that the aggregation-prone, partly folded forms are present in dynamic equilibrium with the native protein at significant concentrations, even under conditions where the native state is thermodynamically stable, and could be important determinants of the amyloidogenic properties of the variants and the slow deposition of fibrils observed at 4 °C.

The previously characterized kinetic and equilibrium partly folded intermediates of lysozymes and the α -lactalbumins all have persistent structure in the α -domain but lack stable, native-like structure in the β -domain^{20,21,31}. Based on the present results, we propose a model for lysozyme fibrillogenesis in which association of the partly folded forms of the variants occurs through the unstable β -domain (Fig. 7). In support of this, a peptide corresponding to the β -sheet region of hen lysozyme has been shown to form extensive intermolecular β -structure³⁴. The development of stable β -structure through such intermolecular association could then act as a template for the progressive recruitment of polypeptide chain into the nascent fibril, with the growth of hydrogen-bonded β -structure providing the context³⁵ for the deposition of poly-

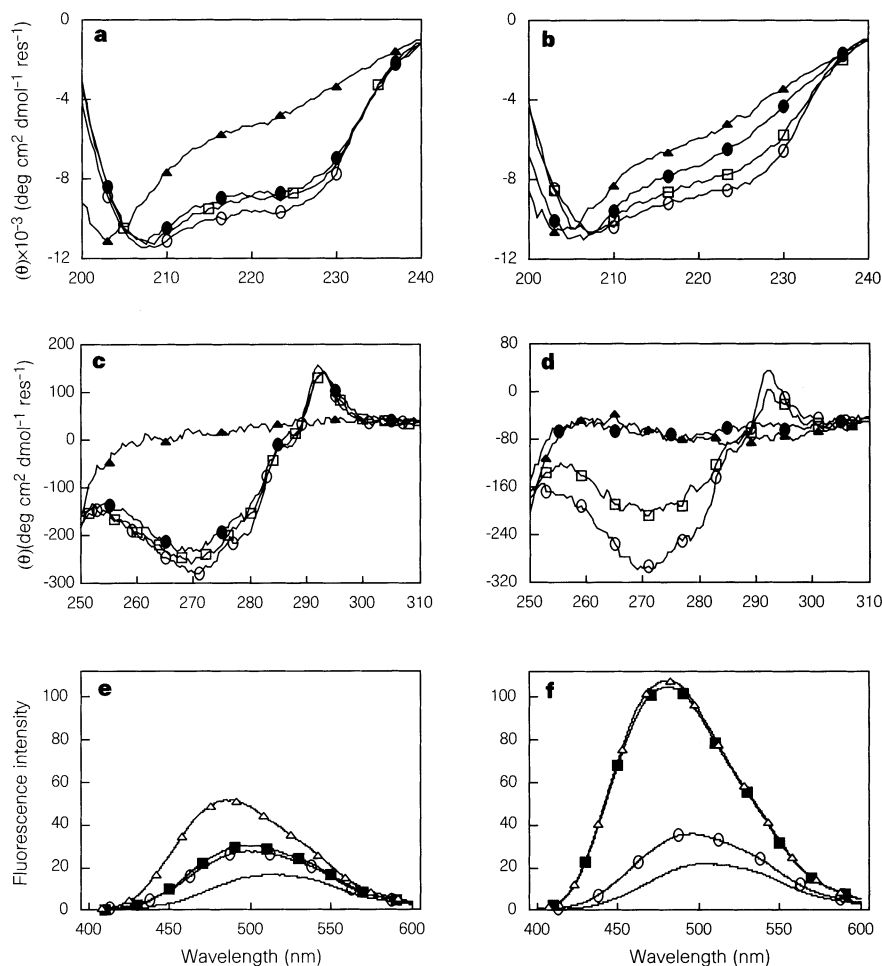


Figure 5 Thermal denaturation of wild-type and Asp67His human lysozymes. Far-UV (a) and near-UV (c) CD spectra for wild-type human lysozyme and far-UV (b) and near-UV (d) CD spectra for the Asp67His variant lysozyme, all obtained in water at pH 5.0 and collected at 20 (○), 60 (□), 70 (●) and 95°C (▲). Binding of 1-anilino-naphthalenesulphonic acid (ANS) to the proteins at 20°C (e) and at the

midpoint of thermal denaturation, T_m (f). The midpoint of thermal denaturation was 74 °C for wild-type human lysozyme and 62 °C for the Asp67His and Ile56Thr variants. Fluorescence intensity (arbitrary units) is shown for ANS-containing buffer solution (solid line), wild-type lysozyme (○), Asp67His lysozyme (■) and Ile56Thr lysozyme (Δ). $\langle \theta \rangle$, molar ellipticity.

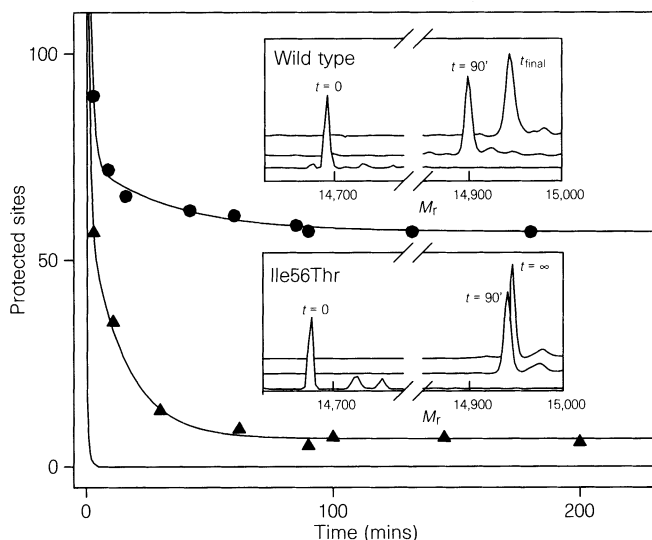


Figure 6 Kinetic profiles of hydrogen exchange at pH 5.0, 37 °C, for wild-type human lysozyme (circles) and Ile56Thr variant (triangles) monitored by ESI-MS. The exchange profile for the Asp67His variant is very similar to that shown here for the Ile56Thr variant. The plain black line is the simulated curve predicted⁴⁸ for a completely unstructured peptide with the sequence of human lysozyme at pH 5.0 and 37 °C. The two inserts represent mass spectra obtained for the wild-type and variant protein before exposure to D₂O ($t = 0$), 90 min after the initiation of exchange ($t = 90'$), and after heating to 70 °C for 15 min to facilitate complete exchange (t_{final}). Data were corrected for the residual 10% H₂O.

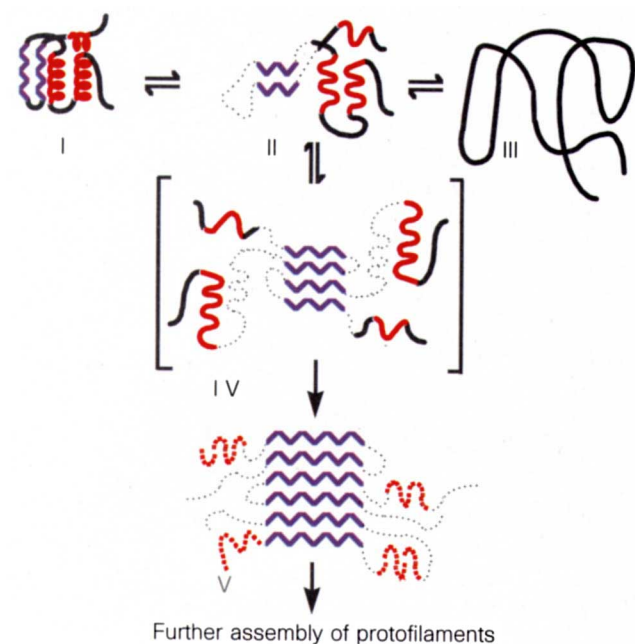


Figure 7 Proposed mechanism for lysozyme amyloid fibril formation. Blue, β -sheet structure; red, helical structure; dotted lines, undefined structure. A partly folded, molten globule-like form of the protein (II), distinct from the native (I) and denatured (III) states, self-associates through the β -domain (IV) to initiate fibril formation. This provides the template for further deposition of protein and for the development of the stable, mainly β -sheet, core structure of the fibril (V). The undefined regions in V represent the possibility that not all of the polypeptide sequence is involved in the cross- β structure. The nature of this residual structure in V is not known, and the figure is not intended to represent any defined secondary structural type (see text).

peptide chain in the stable cross- β fold. The FTIR data indicate that fibrillogenesis involves an increase in β -sheet structure; conversion of α - to β -structure will be easier in the molten globule state than the native state because of the much lower cooperativity of the unfolding process²³.

Mechanism of amyloid fibril formation

All amyloid fibrils have similar morphological and tinctorial characteristics and are predominantly β -sheet structures, indicating that a conformational change, involving a helix-to-sheet transition in some proteins, occurs during fibril formation¹³. As in lysozyme amyloidosis, amino-acid substitutions responsible for amyloid formation in immunoglobulin light chain⁸ and transthyretin variants¹¹ affect the stability of the proteins and their tendency to aggregate. It has been suggested that molten globule states are critical in protein folding and related structural transitions^{36,37}. We propose that transient population of the amyloidogenic proteins in a molten globule-like state that lacks global cooperativity is an important feature of the conversion from the soluble to the fibrillar form. The structure of a domain of the prion protein PrP(121–231)³⁸ also demonstrates that residues for which mutations are associated with prion disease are involved in maintenance of the hydrophobic core. It has also been suggested that the conversion of the cellular form to the infectious form, which involves helix-to-sheet conversion, may be initiated by the β -sheet elements of the native structure³⁸. There is no evidence for infectivity of other types of amyloidosis or for conversion of non-amyloidogenic wild-type proteins by exposure to amyloidogenic variants. Nevertheless, the mechanism we have described for lysozyme amyloidosis (Fig. 7), proceeding from the soluble forms of amyloidogenic precursor

proteins through a transient population of intermediates with the structural characteristics of molten globules, and on to intermolecular β -sheet association, may occur generally in the amyloidoses. *Note added in proof:* After submission of this manuscript Funahashi *et al.*⁴⁹ reported that the crystal structure of Ile56Thr variant lysozyme is similar to that of wild-type human lysozyme, as shown here. Their physicochemical studies also demonstrate reduced protein stability and altered folding kinetics, strongly supporting the idea that partly folded intermediates play an important role in lysozyme fibril formation. □

Methods

Lysozyme expression. Human wild-type and Asp67His variant lysozyme cDNAs were amplified from macrophage RNA of the Asp67His proband. The 5' primer, CTTGGATCCCTAGGACTCTGACCTAGCAGT, contained a *Bam*HI site and targeted sequence in the untranslated region of the cDNA. The 3' primer, NNNNNNTCTAGATTACACTCCACAACCTTG, contained an *Xba*I site and 6 random nucleotides at its 5' end to facilitate cleavage³⁹. The Ile56Thr variant sequence was obtained by *in vitro* mutagenesis of wild-type cDNA (pAlter system, Promega). The three cDNAs were cloned into the *Bam*HI/*Xba*I sites of pBacPAK8, transfected into Sf9 cells, and recombinant baculoviruses were selected and amplified (Clontech). Lysozyme was detected⁴⁰ in medium from infected cells; spinner cultures of Hi5 and Sf9 cells, infected at multiplicity of infections from 1 to 15, yielded 2–20 mg l⁻¹.

Isolation and characterization of recombinant lysozymes. Lysozymes were isolated by cation-exchange chromatography (Macrorep S, BioRad) and FPLC gel filtration (Superose 12, Pharmacia), and gave single bands on reduced SDS 8–18% gradient PAGE (Pharmacia ExcelGel) stained with silver. Lysozyme enzyme kinetics were determined with penta-*N*-acetyl- β -chitopentaoside⁴¹. For electron microscopy, protein diluted in water was placed on a formvar-coated grid and negatively stained with 2% sodium phosphotungstate.

Crystal-structure determination. All crystals were grown by vapour diffusion at 20°C; wild-type lysozyme from 30 mM sodium phosphate, 2.5 M NaCl, pH 4.9, Asp67His from 0.1 M ammonium sulphate, 30% PEG 8000 and Ile56Thr from 0.16 M ammonium sulphate, 24% PEG 8000. Drops initially contained equal volumes of protein (10 mg ml⁻¹ in 10 mM HEPES, 0.4–0.5 M LiCl, pH 7.1–8.0) and reservoir buffer. X-ray data were collected at 15°C using a MAR RESEARCH image plate, mounted on a Rigaku rotating anode X-ray generator. Data processing and reduction were performed with the DENZO and SCALEPACK programs⁴². The CCP4 suite of programs⁴³ was used for map calculation and coordinate analysis. The structures were refined using cycles of restrained molecular dynamics and positional refinement in X-PLOR 3.1 (ref. 44) and manual fitting with the interactive graphics programme O⁴⁵. Crystallographic data statistics are given in Table 3. Recombinant wild-type human lysozyme data were collected as a control set. The initial 2F_o – F_c map for the Ile56Thr variant structure was produced with phases calculated from the refined model of recombinant wild-type human lysozyme¹⁸. The structure of Asp67His lysozyme was solved by molecular replacement using X-PLOR⁴⁴. The solution indicated changes in the conformation of the β -domain (regions 45–54 and 66–75). The structure was rebuilt manually and refined with cycles of molecular dynamics and model building guided by interpretation of electron density maps. Figures were generated with O⁴⁵ and a version of MOLSCRIPT⁴⁶ modified by R. Esnouf.

Thermal stability. Melting temperatures were determined by placing wild-type and variant lysozymes at 2.5 μ g ml⁻¹ in 20 mM HEPES, 100 mM LiCl, pH 7.23, containing 1% (w/v) bovine serum albumin, for 15 min at the temperatures shown, then cooling to 21°C for 15 min, before enzyme assay⁴⁷ at 21°C.

Infrared spectroscopy. Infrared spectra of proteins (~5 mg ml⁻¹) dissolved in D₂O buffer containing 20 mM Tris-HCl, pH 7.0 (uncorrected for deuterium effects) were collected (Bruker IFS-55 spectrometer, 2 cm⁻¹ resolution) before and after heating to induce unfolding and fibril formation.

Recovery of active lysozyme from *ex vivo* lysozyme amyloid fibrils. Amyloid fibrils were isolated by water extraction from amyloidotic liver tissue of a patient with the Asp67His lysozyme gene mutation who underwent emergency liver transplantation following spontaneous rupture of the liver. Lyophilized fibrils were incubated for 72 h in 6 M guanidine HCl, pH 6.7, with or without 0.1% (w/v) 2-mercaptoethanol, then centrifuged to remove

insoluble material. The supernatants were fractionated by FPLC gel filtration (Superose 12, Pharmacia) eluted with the corresponding solvent; the main peak in each case, composed of monomeric lysozyme, was pooled and dialysed against H₂O, pH 3.8. Lysozyme enzyme activity was quantified⁴⁰, and the molecular mass of the solubilised protein was determined by ESI-MS²⁴. The elution volume (*V*_e) of lysozyme recovered in the presence of mercaptoethanol was significantly lower than that obtained without reduction, corresponding to the expected larger volume of unfolded lysozyme without disulphide bridges, confirming that reduction had occurred. This material did not recover enzyme activity and gave no signal in the mass spectrometer, presumably because of its propensity to aggregate. Natural *ex vivo* wild-type lysozyme dissolved in 6 M guanidine-HCl, pH 6.7, and run on the same column as a control, eluted with the same *V*_e as the Asp67His lysozyme from the amyloid fibrils.

Circular dichroism. Spectra were collected at 1-nm intervals using a JASCO J720 spectropolarimeter with 1 mm and 10 mm path-length quartz cuvettes in a temperature-controlled housing, over the wavelength ranges 190–250 nm and 250–360 nm respectively. The protein samples were at 0.22 mg ml⁻¹ in H₂O, pH 5.0, based on *E*₂₈₀^{1%} for 1 cm path length = 25.5.

ANS binding and fluorescence. Proteins at 0.2 mg ml⁻¹ in 50 mM sodium acetate, pH 5.0, with final ANS concentration 0.1 mg ml⁻¹, were analysed in a Perkin Elmer luminescence spectrometer LS50B with a temperature-controlled cell; excitation wavelength, 385 nm; total fluorescence emission monitored between 400 and 600 nm.

Deuterium exchange and mass spectrometry. Proteins were washed extensively in water, pH 3.8, then equilibrated in water, pH 5.0, at 20 μM for determination of mass spectra³³. Hydrogen exchange was initiated by a 10-fold dilution from protein in H₂O at pH 5.0 and 37 °C into D₂O at pH 5.0 (uncorrected for deuterium effects) and 37 °C.

Received 12 September 1996; accepted 27 January 1997.

1. Pepys, M. B. in *Santer's Immunologic Diseases* (eds Frank, M. M., Austen, K. F., Claman, H. N. & Unanue, E. R.) 637–655 (Little, Brown and Company, Boston, 1994).
2. Tan, S. Y. & Pepys, M. B. Amyloidosis. *Histopathology* 25, 403–414 (1994).
3. Glenner, G. G. Amyloid deposits and amyloidosis—the β-fibrilloses. *N. Engl. J. Med.* 302, 1283–1292 (1980).
4. Blake, C. C. F. & Serpell, L. C. Synchrotron X-ray studies suggest that the core of the transthyretin amyloid fibril is a continuous β-sheet helix. *Structure* 4, 989–998 (1996).
5. Fraser, P. E. *et al.* Fibril formation by primate, rodent and Dutch-hemorrhagic analogues of Alzheimer β-protein. *Biochemistry* 31, 10716–10723 (1992).
6. Goldfarb, L. G., Brown, P., Haltia, M., Ghiso, J. & Frangione, B. Synthetic peptides corresponding to different mutated regions of the amyloid gene in familial Creutzfeldt-Jakob disease show enhanced *in vitro* formation of morphologically different amyloid fibrils. *Proc. Natl Acad. Sci. USA* 90, 4451–4454 (1993).
7. Abrahamson, M. & Grubb, A. Increased body temperature accelerates aggregation of the Leu-68-Gln mutant cystatin C, the amyloid-forming protein in hereditary cystatin C amyloid angiopathy. *Proc. Natl Acad. Sci. USA* 91, 1416–1420 (1994).
8. Hurler, M. R., Helms, L. R., Li, L., Chan, W. & Wetzel, R. A role for destabilizing amino acid replacements in light-chain amyloidosis. *Proc. Natl Acad. Sci. USA* 91, 5446–5450 (1994).
9. Maury, C. P. J., Nurmiaho-Lassila, E.-L. & Rossi, H. Amyloid fibril formation in gelsolin-derived amyloidosis. Definition of the amyloidogenic region and evidence of accelerated amyloid formation of mutant Asn-187 and Tyr-187 gelsolin peptides. *Lab. Invest.* 70, 558–564 (1994).
10. Yamada, T., Kluge-Beckerman, B., Liepnicks, J. J. & Benson, M. D. Fibril formation from recombinant human serum amyloid A. *Biochim. Biophys. Acta* 1226, 323–329 (1994).
11. McCutchen, S. L., Lai, Z., Mirog, G. J., Kelly, J. W. & Colon, W. Comparison of lethal and nonlethal transthyretin variants and their relationship to amyloid disease. *Biochemistry* 34, 13527–13536 (1995).
12. Lansbury, P. T. Jr *et al.* Structural model for the β-amyloid fibril based on interstrand alignment of an antiparallel-sheet comprising a C-terminal peptide. *Nature Struct. Biol.* 2, 990–998 (1995).
13. Kelly, J. W. Alternative conformations of amyloidogenic proteins govern their behaviour. *Curr. Opin. Struct. Biol.* 6, 11–17 (1996).
14. Booth, D. R. *et al.* Hereditary hepatic and systemic amyloidosis caused by a new deletion/insertion mutation in the apolipoprotein A1 gene. *J. Clin. Invest.* 98, 2714–2721 (1996).
15. Pepys, M. B. *et al.* Human lysozyme gene mutations cause hereditary systemic amyloidosis. *Nature* 362, 553–557 (1993).
16. Blake, C. C. F. *et al.* Structure of hen egg-white lysozyme. *Nature* 206, 757–761 (1965).
17. Blake, C. C., Pulford, W. C. & Artymiuk, P. J. X-ray studies of water in crystals of lysozyme. *J. Mol. Biol.* 167, 693–723 (1983).

18. Artymiuk, P. J. & Blake, C. C. F. Refinement of human lysozyme at 1.5 Å resolution analysis of non-bonded and hydrogen-bond interactions. *J. Mol. Biol.* 152, 737–762 (1981).
19. McKenzie, H. A. & White, F. H. Jr Lysozyme and alpha-lactalbumin: structure, function, and interrelationship. *Adv. Protein Chem.* 41, 173–315 (1991).
20. Radford, S. E., Dobson, C. M. & Evans, P. A. The folding of hen lysozyme involves partially structured intermediates and multiple pathways. *Nature* 358, 302–307 (1992).
21. Radford, S. E. & Dobson, C. M. Insights into protein folding using physical techniques: studies of lysozyme and α-lactalbumin. *Phil. Trans. R. Soc. Lond. B* 348, 17–25 (1995).
22. Kuwajima, K. The molten globule state as a clue for understanding the folding and cooperativity of globular-protein structure. *Proteins Struct. Funct. Genet.* 6, 87–103 (1989).
23. Pitsyn, O. B. Molten globule and protein folding. *Adv. Protein Chem.* 47, 83–229 (1995).
24. Fenn, J. B., Mann, M., Meng, C. K., Wong, S. F. & Whitehouse, C. M. Electrospray ionization for mass spectrometry of large biomolecules. *Science* 246, 64–71 (1989).
25. Shih, P., Holland, D. R. & Kirsch, J. F. Thermal stability determinants of chicken egg-white lysozyme core mutants: hydrophobicity, packing volume, and conserved buried water molecules. *Protein Sci.* 4, 2050–2062 (1995).
26. Puchtler, H., Sweat, F. & Levine, M. On the binding of Congo red by amyloid. *J. Histochem. Cytochem.* 10, 355–364 (1995).
27. Harrison, R. F. *et al.* 'Fragile' liver and massive hepatic haemorrhage due to hereditary amyloidosis. *Gut* 38, 151–152 (1996).
28. Stott, K., Blackburn, J. M., Butler, P. J. & Perutz, M. Incorporation of glutamine repeats makes protein oligomerize: implications for neurodegenerative diseases. *Proc. Natl Acad. Sci. USA* 92, 6509–6513 (1995).
29. Nelson, S. R., Lyon, M., Gallagher, J. T., Johnson, E. A. & Pepys, M. B. Isolation and characterization of the integral glycosaminoglycan constituents of human amyloid A and monoclonal light-chain amyloid fibrils. *Biochem. J.* 275, 67–73 (1991).
30. Haezebrouck, P. *et al.* An equilibrium partially folded state of human lysozyme at low pH. *J. Mol. Biol.* 246, 382–387 (1995).
31. Wu, L. C., Peng, Z.-y. & Kim, P. S. Bipartite structure of the α-lactalbumin molten globule. *Nature Struct. Biol.* 2, 281–286 (1995).
32. Eyles, S. J., Radford, S. E., Robinson, C. V. & Dobson, C. M. Kinetic consequences of the removal of a disulfide bridge on the folding of hen lysozyme. *Biochemistry* 33, 13038–13048 (1994).
33. Robinson, C. V. *et al.* Conformation of GroEL-bound alpha-lactalbumin probed by mass spectrometry. *Nature* 372, 646–651 (1994).
34. Yang, J. J., Pitkeathly, M. & Radford, S. E. Far-UV circular dichroism reveals a conformational switch in a peptide fragment from the beta-sheet of hen lysozyme. *Biochemistry* 33, 7345–7353 (1994).
35. Minor, D. L. Jr & Kim, P. S. Context-dependent secondary structure formation of a designed protein sequence. *Nature* 380, 730–734 (1996).
36. Dobson, C. M. Finding the right fold. *Nature Struct. Biol.* 2, 513–517 (1995).
37. Bychkova, V. E. & Pitsyn, O. B. Folding intermediates are involved in genetic diseases? *FEBS Lett.* 359, 6–8 (1995).
38. Riek, R. *et al.* NMR structure of the mouse prion protein domain PrP (121–321). *Nature* 382, 180–182 (1996).
39. Chung, L. P., Keshav, S. & Gordon, S. Cloning the human lysozyme cDNA: inverted Alu repeat in the mRNA and *in situ* hybridization for macrophages and Paneth cells. *Proc. Natl Acad. Sci. USA* 85, 6227–6231 (1988).
40. Osserman, E. F. & Lawlor, D. P. Serum and urinary lysozymes (muramidase) in monocytic and monomyelocytic leukemia. *J. Exp. Med.* 124, 921–951 (1996).
41. Nanjo, F., Sakai, K. & Usui, T. p-nitrophenol pent-N-acetyl-beta-chitopentaoside as a novel synthetic substrate for the colorimetric assay of lysozyme. *J. Biochem.* 104, 255–258 (1988).
42. Otwinski, Z. in *Proceedings of the CCP4 Study Weekend* (eds Sawyer, L., Isaacs, N. & Bailey, S.) (SERC Daresbury Laboratory, Warrington, UK, 1993).
43. CCP4 The CCP4 Suite: programs for protein crystallography. *Acta Crystallogr. D* 50, 760–763 (1994).
44. Brünger, A. T. *X-PLOR manual version 3.0* (Yale University, New Haven, CT, 1992).
45. Jones, T. A., Zou, J.-Y., Cowan, S. W. & Kjeldgaard, M. Improved methods for the building of protein models in electron density maps and the location of errors in these models. *Acta Crystallogr. A* 74, 110–119 (1991).
46. Kraulis, P. J. MOLSCRIPT: a program to produce both detailed and schematic plots of protein structures. *J. Appl. Crystallogr.* 24, 946–950 (1991).
47. Perry, L. J. & Wetzel, R. Unpaired cysteine-54 interferes with the ability of an engineered disulfide to stabilize T4 lysozyme. *Biochemistry* 25, 733–739 (1986).
48. Bai, Y., Milne, J. S., Mayne, L. & Englander, S. W. Primary structure effects on peptide group hydrogen exchange. *Proteins Struct. Funct. Genet.* 17, 75–86 (1993).
49. Funahashi, J., Takano, K., Ogasahara, K., Yamagata, Y. & Yutani, K. The structure, stability, and folding process of amyloidogenic mutant human lysozyme. *J. Biochem.* 120, 1216–1223 (1996).

Acknowledgements. We thank G. Merlini for highly purified natural human lysozyme; V. Emons and L. B. Lovat for electron microscopy; K. Harlos and L. C. Serpell for help with X-ray data collection; S. Lee and M. Bartlam for assistance with figures; I. D. Kerr and C. P. Ponting for sequence analysis; and A. K. Soutar for discussions. This work was supported by MRC programme and project grants (M.B.P., P.N.H. and C.C.F.B.), the EU (V.B.), the Royal Society (S.E.R. and C.V.R.), the Oxford Centre for Molecular Sciences (funded by the BBSRC, EPSRC and MRC), the Alzheimer Association of Ontario (P.E.F.) and an international research scholars award from the Howard Hughes Medical Institute (C.M.D.).

Correspondence should be addressed to M.B.P. (e-mail: mpepys@rmps.ac.uk). Requests for molecular reagents should be addressed to D.R.B. (e-mail: dbooth@rmps.ac.uk) and for biophysical data to M.S. (e-mail: margie@bioch.ox.ac.uk). The variant-lysozyme coordinates have been deposited in the Protein Data Bank, accession no. 1LOZ for Ile56Thr and 1LYY for Asp67His.